(12) INTERNATIONAL APPLICATION PUBLISHED UNDER THE PATENT COOPERATION TREATY (PCT)

(19) World Intellectual Property Organization
International Bureau

(43) International Publication Date
4 July 2002 (04.07.2002)

PCT

(10) International Publication Number
WO 02/052331 A2

(51) International Patent Classification[7]: G02B 27/44, 21/00

(21) International Application Number: PCT/US01/44159

(22) International Filing Date:
14 November 2001 (14.11.2001)

(25) Filing Language: English

(26) Publication Language: English

(30) Priority Data:
09/747,788 22 December 2000 (22.12.2000) US

(71) Applicant: CDM OPTICS, INCORPORATED [US/US]; Suite 2110, 4001 Discovery Drive, Boulder, CO 80303-7816 (US).

(72) Inventor: DOWSKI, Edward, Raymond, Jr.; 307 East Cleveland Street, Lafayette, CO 80026 (US).

(74) Agents: BALES, Jennifer, L. et al.; Macheledt Bales LLP, Mountain View Plaza, 1520 Euclid Circle, Lafayette, CO 80026-1250 (US).

(81) Designated States *(national)*: AE, AG, AL, AM, AT, AU, AZ, BA, BB, BG, BR, BY, BZ, CA, CH, CN, CO, CR, CU, CZ, DE, DK, DM, DZ, EE, ES, FI, GB, GD, GE, GH, GM, HR, HU, ID, IL, IN, IS, JP, KE, KG, KP, KR, KZ, LC, LK, LR, LS, LT, LU, LV, MA, MD, MG, MK, MN, MW, MX, MZ, NO, NZ, PL, PT, RO, RU, SD, SE, SG, SI, SK, SL, TJ, TM, TR, TT, TZ, UA, UG, UZ, VN, YU, ZA, ZW.

(84) Designated States *(regional)*: ARIPO patent (GH, GM, KE, LS, MW, MZ, SD, SL, SZ, TZ, UG, ZW), Eurasian patent (AM, AZ, BY, KG, KZ, MD, RU, TJ, TM), European patent (AT, BE, CH, CY, DE, DK, ES, FI, FR, GB, GR, IE, IT, LU, MC, NL, PT, SE, TR), OAPI patent (BF, BJ, CF, CG, CI, CM, GA, GN, GQ, GW, ML, MR, NE, SN, TD, TG).

[Continued on next page]

(54) Title: WAVEFRONT CODED IMAGING SYSTEMS

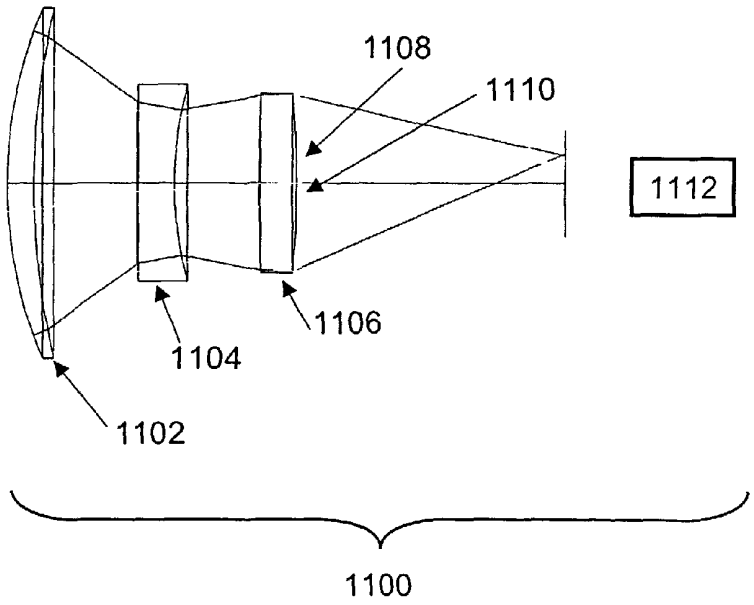

(57) Abstract: The present invention provides improved Wavefront Coding imaging apparatus (100, 800, 1100) and methods composed of optics (102, 802, 1102), wavefront coding (104, 806, 1110), detection (106), and processing (112, 810, 1112) of the detected image. The optics are constructed and arranged to have the characteristic that the transverse ray intercept curves form substantially straight, sloped lines. The wavefront coding corrects for known or unknown amounts of "misfocus-like" aberrations by altering the optical transfer function of the imaging apparatus in such a way that the altered optical transfer function is substantially insensitive to aberrations. Post processing then removes the effect of the coding, except for the invariance with regard to aberrations, producing clear images.

WO 02/052331 A2

Published:

— *without international search report and to be republished upon receipt of that report*

For two-letter codes and other abbreviations, refer to the "Guidance Notes on Codes and Abbreviations" appearing at the beginning of each regular issue of the PCT Gazette.

WAVEFRONT CODED IMAGING SYSTEMS

BACKGROUND OF THE INVENTION

FIELD OF THE INVENTION:

This invention relates to apparatus and methods for optical design based on wavefront coding combined with post processing of images.

DESCRIPTION OF THE PRIOR ART:

U.S. Patent No. 5,748,371, issued May 5, 1998 and entitled "Extended Depth of Field Optical Systems," is a relevant reference.

Traditional optical design is based on the premise that the only major components of the imaging system are the optics and detector. The detector can be analog (e.g. film) or a digital (e.g. CCD, CMOS etc.) detector. Traditional image processing techniques performed on an image are performed after the image is formed. Examples of traditional image processing include edge sharpening and color filter array (CFA) color interpolation. Traditional optics are therefore designed to form images at the detector that are sharp and clear over a range of field angles, illumination wavelengths, temperatures, and focus positions. Consequently, a trade off is made between forming good images, which requires optical designs that are larger, heavier, and contain more optical elements than are desirable, and modifying the design in order to

reduce size, weight, or the number of optical elements, which results in loss of image quality.

A need remains in the art for improved optical designs which produce good images with systems that are smaller, lighter, and contain fewer elements then those based on traditional optics.

SUMMARY OF THE INVENTION

Optical design based on Wavefront Coding enables systems that can be smaller, lighter, and contain fewer optical elements than those based on traditional optics. Wavefront Coding systems share the task of image formation between optics and digital processing. Instead of the imaging system being primarily composed of optics and the detector, Wavefront Coding imaging systems are composed of optics, detector, and importantly, processing of the detected image. The detector can in general be analog, such as film, or a digital detector. Since processing of the detected image is an integral part of the total system, the optics of Wavefront Coded imaging systems do not need to form sharp and clear images at the plane of the detector. It is only the images after processing that need to be sharp and clear.

Wavefront Coding, in general, corrects for known or unknown amounts of "misfocus-like" aberrations. These aberrations include misfocus, spherical aberration, petzval curvature, astigmatism, and chromatic aberration. System sensitivities to environmental parameters such as temperature and pressure induced aberrations, and mechanical focus related aberrations related to fabrication

error, assembly error, drift, wear, etc., are also reduced with Wavefront Coding. Optical designs based on Wavefront Coding can reduce the effects of these aberrations and result in simpler designs that produce good images.

Optical system designs according to the present invention are improved in that they have the characteristic that the transverse ray intercept curves are substantially straight lines. Unlike traditional optical designs, the transverse ray intercept curves for wavefront coded systems need not have a near zero slope; the slope, which indicates misfocus, may be substantial, because wavefront coding allows the effects due to misfocus to be removed. In actual systems the transverse ray intercept curves should vary mainly in slope over wavelength, field angles, temperature, etc. but need not be exactly straight lines. Some ripple is acceptable. With wavefront coding optical surfaces and post processing, good images can be produced.

BRIEF DESCRIPTION OF THE DRAWINGS

Figure 1 shows a single-lens miniature imaging system according to the present invention.

Figure 2 illustrates a series of transverse ray intercept curves illustrating aberrations at various wavelengths, for the system of Figure 1 with wavefront coding removed.

Figure 3 illustrates distortion curves for the system of Figure 1 with wavefront coding removed.

Figure 4 illustrates modulation transfer functions (MTF) for the system of Figure 1, with wavefront coding removed.

Figure 5 illustrates modulation transfer functions (MTF) for the system of Figure 1, with wavefront coding, but without post processing.

Figure 6 illustrates modulation transfer functions (MTF) for the system of Figure 1, with wavefront coding, both before and after filtering.

Figures 7a and 7b illustrates sampled point spread functions (PSF) for the system of Figure 1, with wavefront coding and after filtering, for two object distances.

Figure 8 shows a low cost microscope objective according to the present invention.

Figure 9 illustrates a series of transverse ray intercept curves illustrating aberrations at various wavelengths, for the system of Figure 8 with wavefront coding removed.

Figure 10 illustrates modulation transfer functions (MTF) for the system of Figure 8, without wavefront coding; with wavefront coding; and with both wavefront coding and filtering.

Figure 11 shows a passive athermalized IR imaging system according to the present invention.

Figure 12 illustrates a series of transverse ray intercept curves illustrating aberrations at various wavelengths, for the system of

Figure 11, without wavefront coding.

Figure 13 illustrates modulation transfer functions (MTF) for the system of Figure 11, without wavefront coding.

Figure 14 illustrates modulation transfer functions (MTF) for the system of Figure 11, with wavefront coding, both with and without filtering.

Figure 15a illustrates transverse ray intercept curves as typically implemented in traditional imaging systems.

Figure 15b shows MTFs for the system of Figure 15a.

Figure 16 illustrates an example of a one dimensional separable filter for use as a post processing element in the present invention.

Figure 17 illustrates the magnitude of the transfer function of the filter of Figure 16.

DETAILED DESCRIPTION OF THE PREFERRED EMBODIMENTS

Figure 1 shows a single-lens miniature imaging system 100 according to the present invention. Lens 102 includes wavefront coding element 104 formed on its second surface. Detector 106 is preceded by an IR filter 108 and cover glass 110. Post processor 112 performs processing on the images captured by detector 106.

The example single-lens imaging system (singlet) 100 is designed to meet the following specifications:

- f = 2.5mm
- F/# = 2.6
- Length < 4.5 mm
- Material: PMMA
- FOV = 50°
- Focus: ∞ - 30cm
- pixel size = 6 μm
- Bayer CFA / 100 % fill factor
- MTF > 40% at 40 lp/mm

The example singlet 100, without Wavefront Coding 104, was designed so that the aberrations that are not corrected by the optical surfaces, namely petzval curvature and axial chromatic aberration, are a type of misfocus. Specifically, petzval curvature is a type of misfocus with field angle, and axial chromatic aberration is misfocus with illumination wavelength. The effect of these aberrations could hypothetically be corrected within small regions of the image plane by changing the focus position. By adding a Wavefront Coding surface, the resulting modulation transfer functions (MTFs) and point spread functions (PSFs) will be insensitive to the focus-like aberrations. However, the MTFs and PSFs will not be the same as an ideal in-focus MTF or PSF from a traditional imaging system. Image processing is required to restore the spatial character of the image and produce a sharp and clear image.

The form of the Wavefront Coding surface used in this example is :

$$S(x,y) = \sum a_i \, \text{sign}(x) \, |x/r_n|^{b_i} + a_i \, \text{sign}(y) \, |y/r_n|^{b_i}$$

where the sum is over the index *i*. Sign(x) = -1 for $x < 0$, +1 for $x \geq 0$. The parameter r_n is a normalized radius value. This particular Wavefront Coding surface is rectangularly separable and allows for fast processing. Other forms of Wavefront Coding surfaces are non-separable, and the sum of rectangularly separable forms. One non-separable form is defined as:

$$S(r,\theta) = \sum r^{a}_{i} \cos(b_i \theta + \phi_i)$$

where the sum is again over the subscript *i*.

There are an infinite number of Wavefront Coding surface forms. The Wavefront Coding surface for singlet 100 in this example is placed at the stop surface (surface 104) and has the parameterized equation:

$$S(x,y) = \sum a_i \, \text{sign}(x) \, |x/r_n|^{b_i} + a_i \, \text{sign}(y) \, |y/r_n|^{b_i}$$

and the parameter values for $i = 1,2,3$ are:

$a_1 = 17.4171, \quad b_1 = 2.9911$

$a_2 = 10.8895, \quad b_2 = 6$

$a_3 = 3.8845, \quad b_3 = 20.1909$

$r_n = 0.459$

Figures 2-4 illustrate the performance of system 100 with wavefront coding element 104 removed, in order to illustrate design requirements and performance. Figure 5 illustrates the performance of system 100 with wavefront coding element 104 in place, but without post processing filter 112. Figure 6 illustrates the performance

improvement with post processing 112. Figures 7a and 7b shows point spread functions for system 100 with both wavefront coding and post processing.

Figure 2 illustrates a series of transverse ray intercept curves illustrating aberrations at various wavelengths, for the system of Figure 1 with wavefront coding surface 104 removed for illustrative purposes. Curves are shown for system 100 at half field angles of 0º, 10º, 20º, and 25º off axis, and for illumination wavelengths of 450 nm, 550 nm, and 650 nm. A slope of zero indicates an in-focus condition. Thus on-axis rays are nearly in focus. But, for off axis field angles, the slopes of the transverse ray intercept curves increase dramatically.

There are numerous traditional methods of designing lenses. Most methods try to balance aberrations in order to improve the off-axis imaging at the expense of on-axis imaging or system simplicity. Traditional design methodologies do not attempt to make the transverse ray intercept curves straight lines. Instead, the traditional goal is to try to minimize the distance of a substantial portion of the transverse ray intercept curves from the horizontal axis. In most traditional systems the ray intercept curves are very different from straight lines, but in general lie closer to the horizontal axis than the off-axis curves shown in Figure 2. In other words, in traditional systems the variation from a straight horizontal line is mainly in the straightness of the line, rather than in its slope.

Figure 15a (prior art) illustrates traditional transverse ray plots. These plots are taken from "Practical Computer Aided Lens Design",

Gregory Hallick Smith, William Bell, Inc., Richmond 1998. Note that the plot for near on axis rays do look similar to straight horizontal lines, and thus produce an in focus image. Refer also to Figure 15b which shows associated MTFs for this system. The MTFs for near on axis rays are good.

But as the rays move further off axis, the plots in Figure 15a quickly deviate from being straight lines. Their associated MTFs in 15b also quickly degrade.

The transverse ray intercept curves of Figure 2 are essentially straight lines through the origin, both on and off axis, and this is a deliberate design goal, because the use of wavefront coding 104 and image processing 112 can bring the captured images into focus, so long as the curves without wavefront coding are essentially straight lines through the origin, even if the lines are significantly sloped. The effect of the slope is removed by adding wavefront coding and post processing.

The aberration petzval curvature gives rise to transverse ray intercept curves, with slopes that are a function of field angle. Axial chromatic aberration gives rise to ray intercept curves with slopes that are a function of illumination wavelength. From Figure 2, both of these features are part of the transverse ray intercept curves in this example design.

Figure 3 illustrates distortion curves for system 100 of Figure 1, with wavefront coding element 104 removed. The distortion is less than 0.2%. If distortion was large enough then additional digital processing

might be required to reposition image points into a non-distorted image. Table 1 lists the optical prescription of this lens, again without the Wavefront Coding surface. Units are in mm, and the total length is 4.1 mm. Aspheric terms describe rotationally symmetric forms of r^{order} with order equal to 4, 6, 8, etc.

Table 1

Surface	Radius	Thickness	Material	Diameter
Obj	Inf	Inf		0
1	2.077	1.7133	PMMA	2
Stop	-2.236	0.6498		1.4
3	Inf	1.1	BK7	3.4
4	Inf	0.55	BK7	3.4
Img		0.1		3.4

Surface	Conic	4th Asph.	6th Asph.	8th Asph.
Obj	0			
1	-1.299	-.000375	-.010932	-.00603
Stop	-3.140	-.01049		
3	0			
4	0			
Img				

Figure 4 illustrates modulation transfer functions (MTF) for system 100 of Figure 1, without wavefront coding element 104. These MTFs correspond to the transverse ray aberration curves of Figure 2. The MTFs are for half field angles 0, 15, and 25 degrees with wavelengths

of 550 nm. The MTFs include the pixel MTF due to the Bayer color filter array detector with six micron pixels and 100% fill factor. The on-axis MTF is essentially diffraction limited. The large drop in MTF off-axis is due to the large amount of petzval curvature that is unavoidable in traditional single lens designs with a large field of view. This singlet without wavefront coding 104 does not meet the MTF specification of greater than 40% modulation at 40 lp/mm for all field angles. But, due to its design for Wavefront Coding, modifying the second surface with a Wavefront Coding surface form 104 will lead to acceptable MTF modulation values when combined with digital processing. By changing the wavefront coding element 104 either more or less sensitivity to misfocus aberrations can be formed.

Figure 5 illustrates modulation transfer functions (MTF) for system 100 of Figure 1, with wavefront coding element 104 in place, but without post processing 112. The system is focused at infinity. The half field angles shown are 0, 15, and 25 degrees. The wavelength is 550 nm. These MTFs have very little variation with field angle due to the addition of the Wavefront Coding surface, as compared to Figure 4. Pixel MTF due to the Bayer CFA has again been included. The Bayer CFA with 6μm 100% fill factor pixels has a Nyquist spatial frequency of about 42 lp/mm. Note that there are purposely no zeros in the MTFs below the detector's Nyquist spatial frequency.

Since the MTFs of Figure 5 do not match a diffraction-limited MTF curve, a blurred image will be directly formed at the detector by this singlet 102. Post processing is needed to correct this.

Figure 6 illustrates modulation transfer functions (MTF) for system 100 of Figure 1, with wavefront coding 104 and after processing 112. Applying a single digital filter in processing block 112 gives the optical/digital MTFs shown in Figure 6. The MTFs before filtering are as shown in Figure 5. The MTFs after processing 112 at the spatial frequency of 40 lp/mm are all above 40% as specified by the design specifications. The level of the MTFs after processing could further be increased beyond that of the traditional diffraction-limited case, but possibly at the expense of a lower signal to noise ratio of the final image.

Figures 7a and 7b illustrate sampled two-dimensional PSFs for system 100 of Figure 1, with wavefront coding 104 and after processing 112. Figure 7a shows the processed PSFs when the object is at infinity. Figure 7b shows the processed PSFs when the object is at 30cm. These PSFs are for 550 nm wavelength and half field angles of 0, 15, and 25 degrees. After filtering, these PSFs have nearly ideal shapes. This singlet 100 when combined with wavefront coding and digital filtering thus easily meets the system specifications.

In the preferred embodiment, processor 112 is a rectangularly separable digital filter. Rectangularly separable filters are more computationally efficient (counting the number of multiply and additions) than full 2D kernel filters. Separable filtering consists of first filtering each row of the image with the 1D row filter and forming an intermediate image. The columns of the intermediate image are then filtered with the 1D column filter to provide the final in-focus image. The separable filter used for this example singlet has the same

filters for rows and columns.

Figure 16 illustrates an example of a one dimensional separable filter 112. Coefficients are represented as real values, but can be quantified into integer values for fixed point computations. The sum of the filter coefficients equals approximately 1. The coefficients were determined with a least squares algorithm by minimizing the squared difference between the filtered wavefront coded OTFs and a desired MTF with a value greater than 40 % at 40 lp/mm. The width of the filtered PSFs of Figures 7a and 7b are also minimized with the least squares algorithm. Changes in the filtered PSFs are minimized in regions away from their central peaks. Figure 17 illustrates the magnitude of the transfer function of the filter of Figure 16. The zero spatial frequency value is 1.

Figure 8 shows a low cost microscope objective 800 according to the present invention. The magnification of objective 800 is 10X, with numerical aperture (N.A.) = 0.15. Lens 802 is aspheric and has focussing power. Aperture stop 804 includes wavefront coding element 806. Processing is accomplished by processing block 810.

Wavefront coding microscope objective 800 is designed to meet the following objectives:

- magnification = 10X
- N.A. = 0.15
- Distortion < 1%
- 7 micron square pixels with 100% fill factor
- VGA grayscale detector

- Optical material: PMMA

The depth of field of traditional microscope objectives is described by the numerical aperture (NA) and the imaging wavelength. The wavefront coding objective can have a depth of field that is independent of the NA of the objective. The depth of field can be large enough to introduce prospective distortion to the final images. Regions of the object that are farther from the objective will appear smaller then regions of the object closer to the objective. Both near and far regions can image clearly with a large depth of field. Since the depth of field of traditional objectives is small prospective distortion is not common with traditional objectives, especially with high NA. Prospective distortion can be reduced or eliminating by designing wavefront coding objectives that are telecentric. In telecentric imaging systems the magnification of the object is independent of the distance to the object.

Figure 9 illustrates a series of transverse ray intercept curves illustrating aberrations at various wavelengths, for system 800 of Figure 8, with wavefront coding element 806 removed. The ray intercept curves of Figure 9 describe the performance of the system at wavelengths 450, 550, and 650 nm for the image field heights of on-axis (0.0mm), 1.2mm, and 2.8mm. Full scale is +/- 100 microns. Notice that each of these ray intercept curves vary mainly in slope, as required by the present invention. I.e., the shape of the curves are essentially the same when the slope components of the curves are not considered. While these plots are not quite as close to perfectly straight lines as those in Figure 2, they can still be considered to be substantially sloped straight lines.

The major aberration apparent in this design is axial chromatic aberration, with a smaller amount of petzval curvature and lateral chromatic aberration. Without Wavefront Coding this lens would image poorly in white light, although it might produce a reasonable image in a single color. Tables 2 and 3 give the optical prescription for this system. Table 3 gives rotationally symmetric aspheric terms for the system.

Table 2

Surface	Radius of curv	Thickness	Material	Diameter	Conic
Obj	Inf	2.45906		0.6357861	0
1	1.973107	1.415926	Acrylic	1.2	-1.680295
2	-2.882275	0.7648311		1.2	-1.029351
Stop	Inf	0.1	Acrylic	0.841	0
4	Inf	25.83517		0.841	0
Img				6.173922	

Table 3

Surface	4th	6th	8th	10th	12th	14th
1	**0.013191**	**-0.22886**	**0.139609**	**-0.250285**	**-0.18807**	**0.193763**
2	**-0.008797**	**0.017236**	**0.007808**	**-0.223224**	**0.160689**	**-0.274339**
Stop	**-0.018549**	**-0.010249**	**-0.303999**	**1.369745**	**11.245778**	**-59.7839958**

Wavefront coding element 806 is placed at aperture stop 804, and is given by the rectangularly separable form of:

$$S(x,y) = \sum a_i \, \text{sign}(x) \, |x/r_n|^{b_i} + a_i \, \text{sign}(y) \, |y/r_n|^{b_i}$$

and the parameter values for $i = 1,2$ are:

$a_1 = 1.486852, \quad b_1 = 3.0$

$a_2 = 3.221235, \quad b_2 = 10.0$

$r_n = 0.419$

Figure 10 illustrates modulation transfer functions (MTF) for system 800 of Figure 8, without wavefront coding, with wavefront coding, and with both wavefront coding and post processing filtering, for illumination at 450 nm. Image field heights are 0.0mm, 1.2 mm, and 2.8 mm.

Figure 11 shows a passive athermalized IR imaging system 1100 according to the present invention. Lens 1102 is composed of silicon. Lens 1104 is composed of germanium. Lens 1106 is composed of silicon. The aperture stop 1108 is at the back surface of lens 1106. Wavefront coding surface 1110 is on the back surface of lens 1106 (at aperture stop 1108). Processing block 1112 processes the image.

Design goals are as follows:

- F/2
- f= 100 mm
- 3 deg half field of view

- Illumination wavelength = 10 microns
- 20 micron square pixels, 100% fill factor
- Silicon & germanium optics
- Aluminum mounts
- Temperature range of -20°C to +70°C

Combined constraints of low F/#, inexpensive mounting material, and wide operating temperature make this design very difficult for traditional optics. Table 4 gives the optical prescription of system 1100.

Table 4

Surface	Radius of curv.	Thickness	Material	Diameter	Conic
Obj	Inf	Inf		0.6357861	0
1	58.6656	5.707297	Silicon	60	0
2	100.9934	22.39862		57.6	0
3	447.046	8.000028	Germanium	32.4	0
4	50.88434	17.54754		32.4	0
5	455.597	7.999977	Silicon	29.5	0
Stop	-115.6064	57.9967		29.5	0
Img				6.173922	

The Wavefront Coding surface for IR system 100 of this example has the parameterized equation:

$$S(x,y) = \sum a_i \, \text{sign}(x) \, |x/r_n|^{b_i} + a_i \, \text{sign}(y) \, |y/r_n|^{b_i}$$

and the parameter values for $i = 1,2$ are:

$a_1 = 16.196742, \quad b_1 = 3.172720$

$a_2 = -311.005659 \ , \ b_2 = 20.033486$

$r_n = 18.314428$

Figure 12 illustrates a series of transverse ray intercept curves illustrating aberrations at various wavelengths, for system 1100 of Figure 11, with wavefront coding element 1110 removed. The ray intercept curves of figure 11 describe the performance of system 1100 at a wavelength of 10 microns, on axis field points for ambient temperatures of +20º C, -20º C, and +70º C. Full scale is +/- 100 microns. Again these plots can be considered to be substantially straight lines. While they have more "wiggle" than the plots of Figures 2 and 9, in each case, if the plot were fitted to the closest straight line, the wiggles would not stray far from the line.

The best way to define what constitutes a "substantially straight line" is to look at the MTFs associated with a particular system before the addition of wavefront coding and without post processing. In figure 13, it can be seen that the on-axis MTF (at +20ºC, meaning essentially no temperature related misfocus) is essentially diffraction limited. The MTFs at other temperatures, though, have reduced performance due to temperature related effects.

Now consider the upper set of MTFs of Figure 14, with wavefront coding and after processing. All of the MTFs are now essentially diffraction limited. Thus the associated transverse ray intercept curves can be considered to be substantially straight lines, since they are close enough to straight to give an ideal MTF.

For other systems, a lower level of performance my be acceptable, and consequently the deviation of the transverse ray intercept curves from a straight line may be larger. Such a situation would result if a fast lens (say F/2) is used with a digital detector, with, say, 10 micron pixels. In 500 nm illumination, the diffraction limited MTF for the optical system would extend to 1000 lp/mm, but the highest spatial frequency that could be measured by the detector would be only 50 lp/mm. Thus, aberrations that alter the highest spatial frequencies of the optics are of no consequence, because they will not be measured by the detector. Note that while the transverse ray intercept curves may have noticeable deviations from a straight line (corresponding to the higher spatial frequencies), the transverse ray intercept curves are still "substantially straight lines" according to our definition, because the resulting MTFs are essentially diffraction limited. The MTFs under consideration are those that correspond to the useful range of the particular system being considered.

Note also that if you took the absolute value of the area between the plot and the best fitting straight line (call it the "wiggle area"), this area would be extremely small compared to the absolute value of the area between the plot and the horizontal axis (over the useful range of the system, though not for the ideal case of +20º C). Thus, again, the plots of Figure 12 can be considered to be substantially straight lines.

The major aberration apparent in this design is temperature related misfocus. Without Wavefront Coding, this lens would image poorly over a range of temperatures, although it would image well at a single temperature.

Figure 13 illustrates on-axis MTF curves for system 1100 without wavefront coding at three temperatures (+20º, -20º, and +70º). Performance is nearly diffraction limited at +20º, but drops dramatically with changes in temperature.

Figure 14 illustrates MTFs for system 1100 of Figure 11, with wavefront coding, both with and without filtering by processing block 1112. The illumination wavelength is 10 microns. The MTFs without filtering are significantly different from diffraction limited MTFs, but vary little with temperature. Thus, processing block 1112 is able to correct the images. The MTFs after filtering are near diffraction limited for all three temperatures (+20º, -20º, and +70º). Filtered MTFs extend only to the Nyquist frequency of the 20 micron detector, or 25 lp/mm.

What is claimed is:

CLAIMS

1. Imaging apparatus (100, 800, 1100) for imaging an object onto a detector (106) comprising:

a lens structure (102, 802, 1102);

the lens structure constructed and arranged to produce transverse ray intercept curves which are substantially sloped straight lines;

a wavefront coding element (104, 806, 1110) positioned between the object and the detector;

the coding element being constructed and arranged to alter the optical transfer function of the imaging apparatus in such a way that the altered optical transfer function is substantially insensitive to focus-related aberrations over a greater range of aberrations than was provided by the unaltered optical transfer function; and

means for post processing (112, 810, 1112);

wherein the coding element affects said alteration to the optical transfer function substantially by affecting the phase of light transmitted by said wavefront coding element.

2. A single lens imaging system (100) for imaging an object onto a detector (106) comprising:

a lens (102) constructed and arranged to produce transverse ray intercept curves which are substantially sloped straight lines;

a wavefront coding element (104) formed on a surface of the lens;

the coding element being constructed and arranged to alter the optical transfer function of the imaging system in such a way that the altered optical transfer function is substantially insensitive to focus-related aberrations over a greater range of aberrations than was provided by the unaltered optical transfer function; and

a post processing element (112);

wherein the coding element affects said alteration to the optical transfer function substantially by affecting the phase of light transmitted by said wavefront coding element.

3. A microscope objective (800) for imaging an object onto a detector comprising:

an element (802) with optical power;

the element with optical power being constructed and arranged to produce transverse ray intercept curves which are substantially sloped straight lines;

a wavefront coding element (806);

the coding element being constructed and arranged to alter the optical transfer function of the microscope objective in such a way that the altered optical transfer function is substantially insensitive to focus-related aberrations over a greater range of aberrations than was provided by the unaltered optical transfer function; and

a post processing element (810);

wherein the coding element affects said alteration to the optical

transfer function substantially by affecting the phase of light transmitted by said wavefront coding element.

4. The apparatus of claim 1, 2, or 3 wherein the aberrations include one or more of the following:

misfocus;
spherical aberration;
petzval curvature;
astigmatism;
field curvature;
chromatic aberration;
temperature induced misfocus aberration;
pressure induced misfocus aberration;
mechanical induced misfocus aberrations.

5. The apparatus of claim 1, 2, or 3 wherein the coding element is formed substantially at an aperture stop of the imaging system.

6. The apparatus of claim 1, 2, or 3 wherein the lens, lens structure or element with optical power comprises an IR imaging system.

7. The apparatus of claim 1, 2, or 3 wherein the post processing means comprises a digital filter.

8. The system of claim 7, wherein the digital filter comprises a rectangularly separable filter.

9. The apparatus of claim 1, 2, or 3 wherein the lens, lens structure or element with optical power comprises a microscope objective.

10. The apparatus of claim 1 or 3 wherein the lens structure or element with optical power comprises a single lens.

11. The apparatus of claim 2 or 10 wherein the coding element is formed on the single lens.

12. The system of claim 2 or 10, wherein the lens length is under 10 mm.

13. The system of claim 12, wherein the lens length is under 5 mm.

14. The microscope objective of claim 2 or 10, wherein the lens is aspheric.

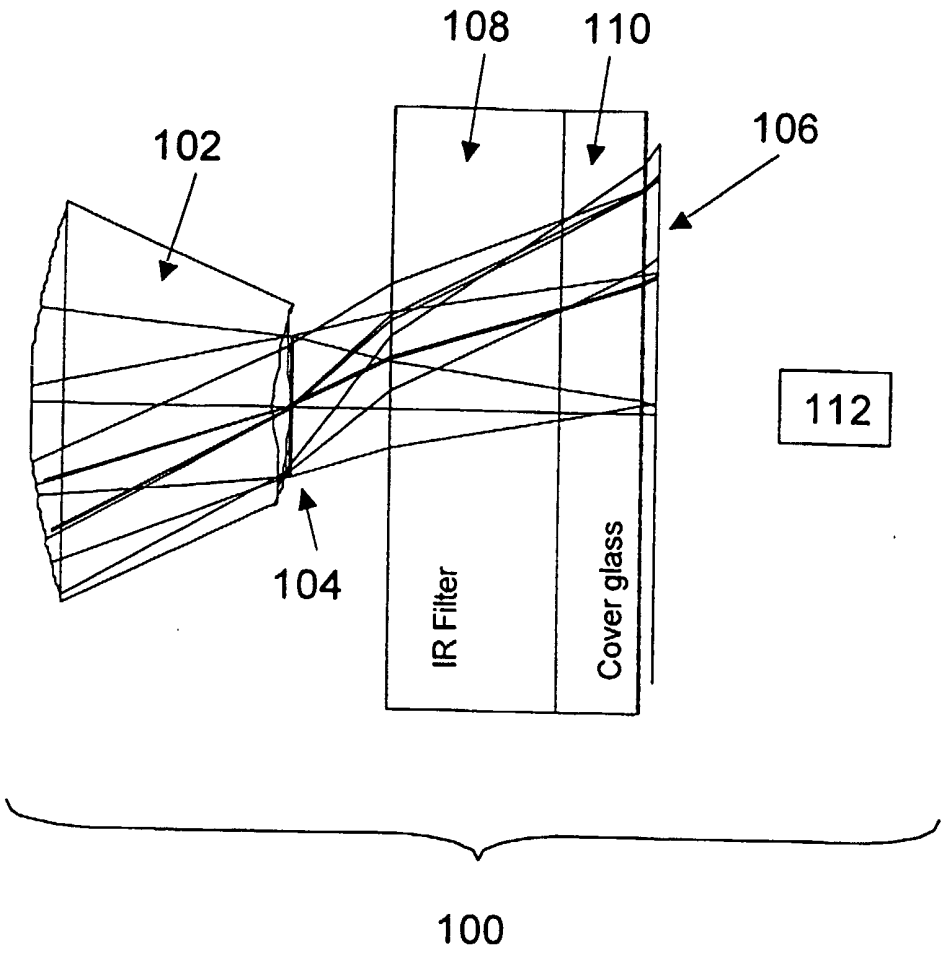

Figure 1

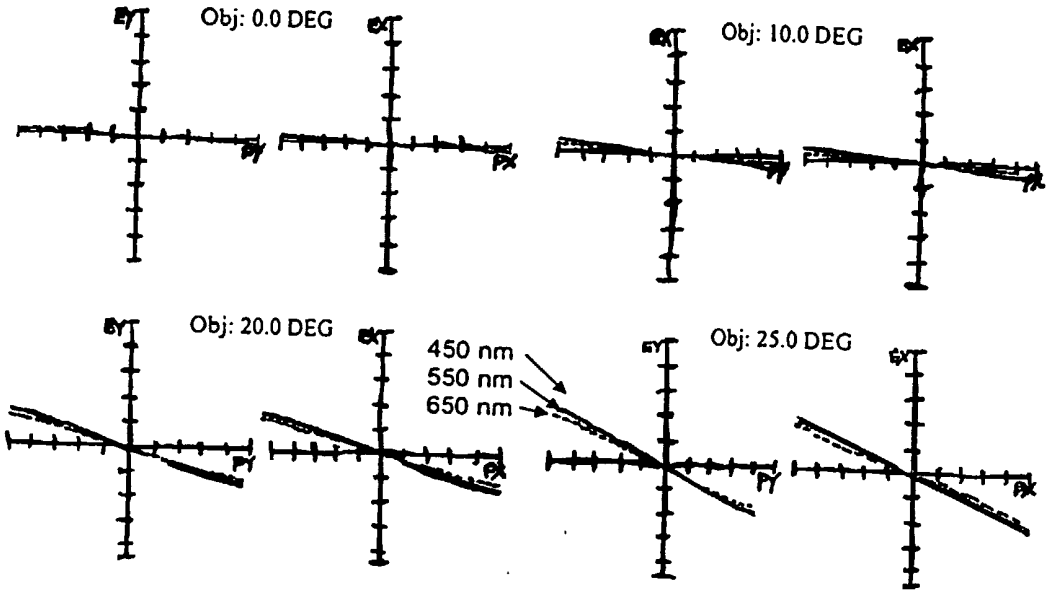
Obj: 0.0 DEG
Obj: 10.0 DEG
Obj: 20.0 DEG
Obj: 25.0 DEG
450 nm
550 nm
650 nm

Figure 2

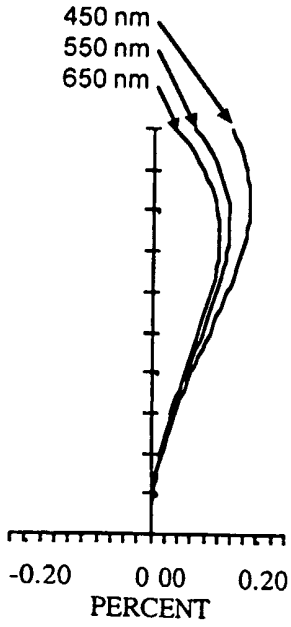

Figure 3

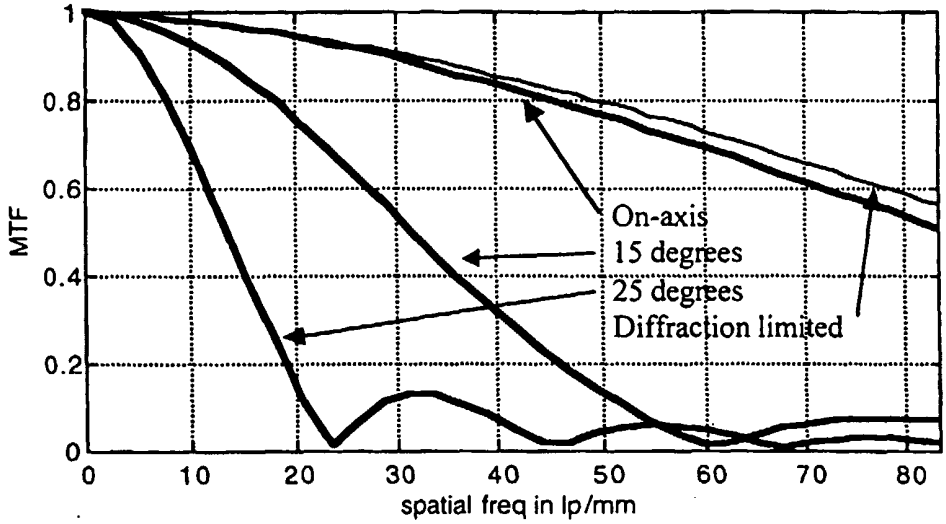
1
0.8
0.6
0.4
0.2
0
MTF
0
10
20
30
40
50
60
70
80
spatial freq in lp/mm
On-axis
15 degrees
25 degrees
Diffraction limited

Figure 4

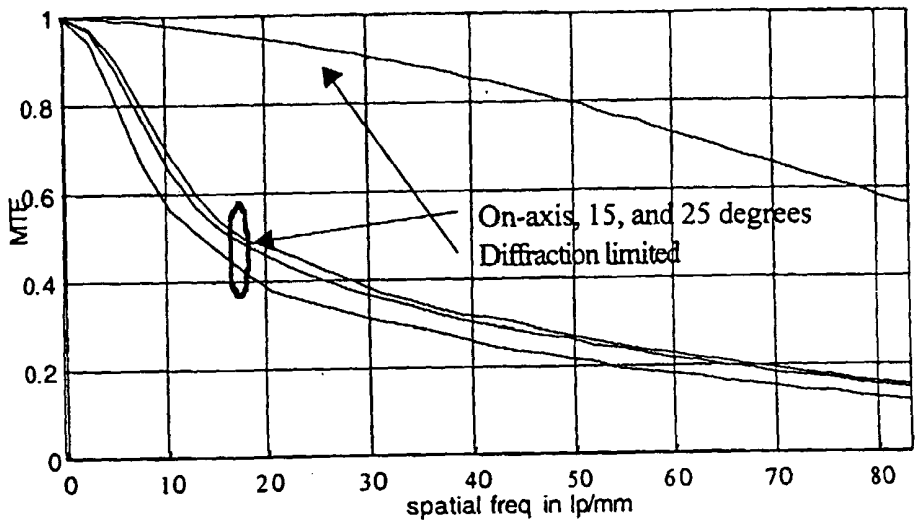
1
0.8
0.6
0.4
0.2
0
MTF
0
10
20
30
40
50
60
70
80
spatial freq in lp/mm
On-axis, 15, and 25 degrees
Diffraction limited

Figure 5

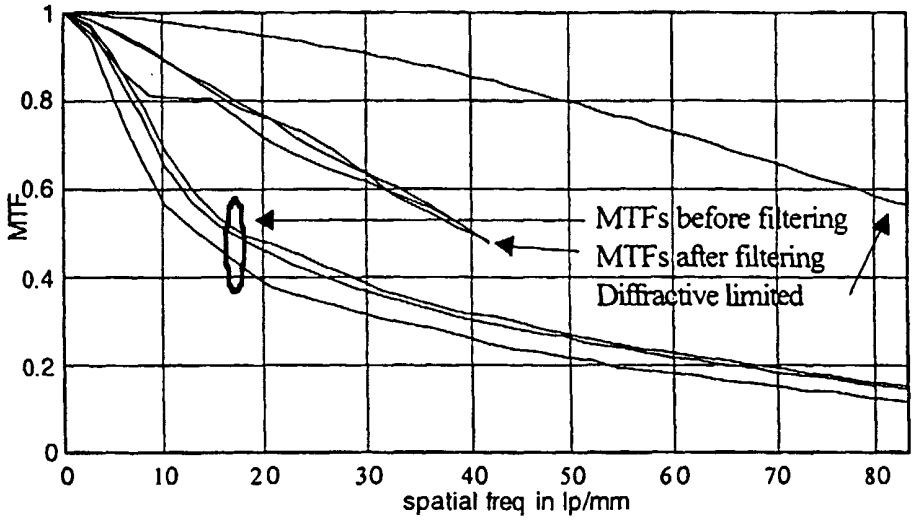
1
0.8
0.6
0.4
0.2
0
MTF
0
10
20
30
40
50
60
70
80
spatial freq in lp/mm
MTFs before filtering
MTFs after filtering
Diffractive limited

Figure 6

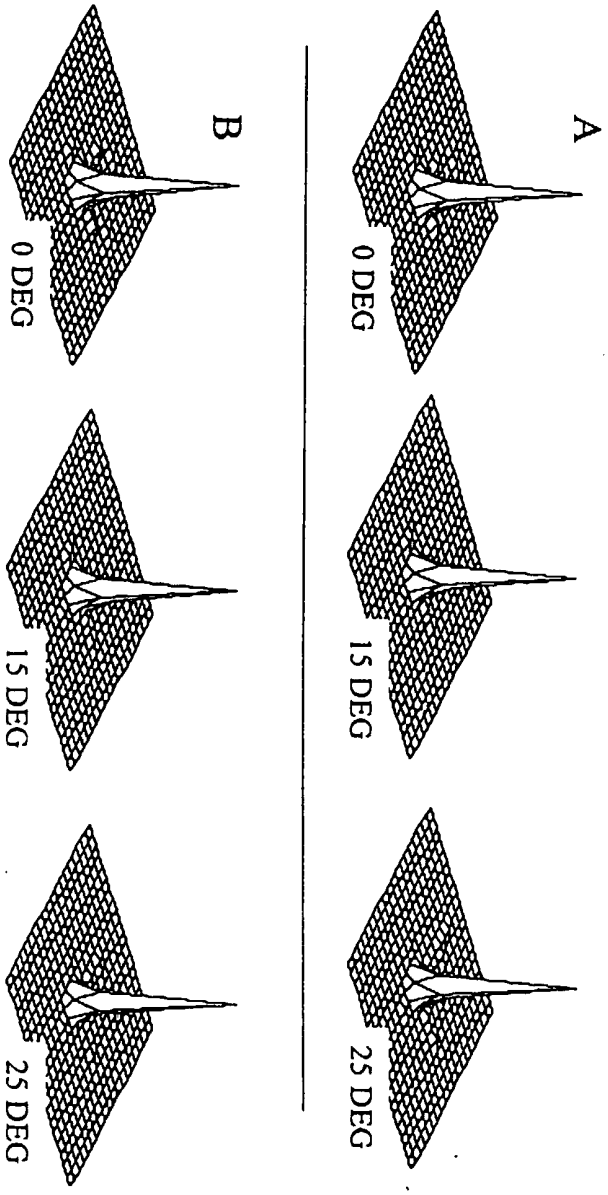

Figure 7

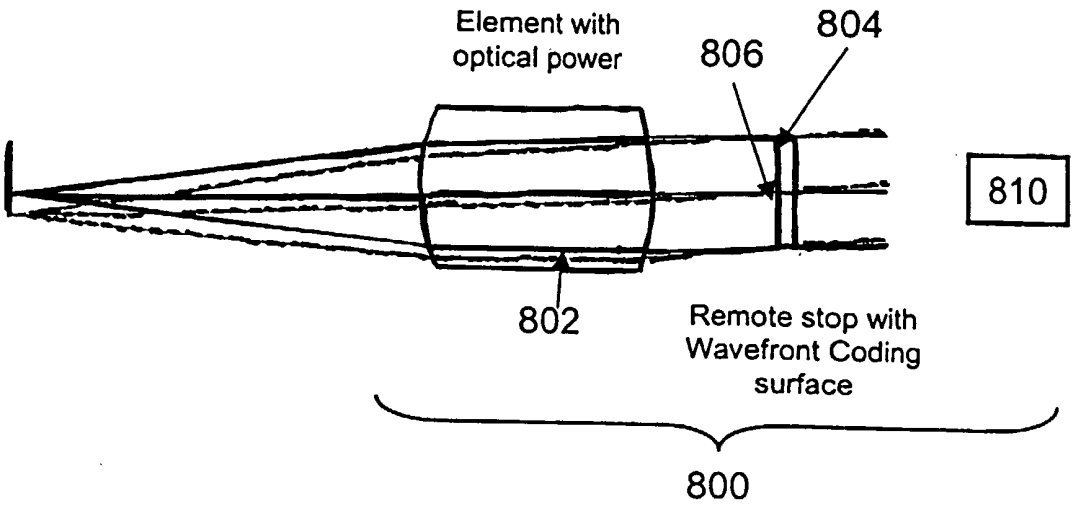
Element with
optical power
806
804
810
802
Remote stop with
Wavefront Coding
surface
800

Figure 8

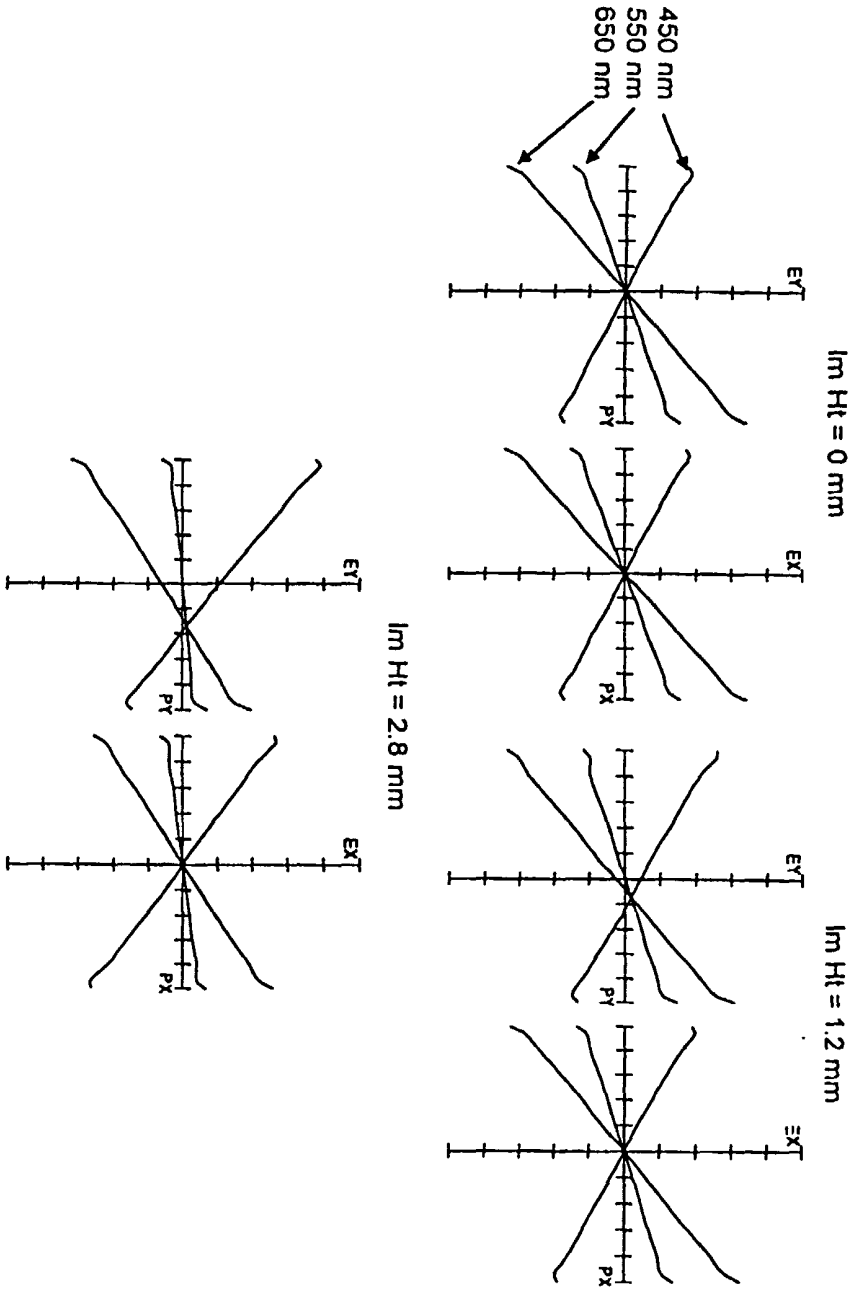

Figure 9

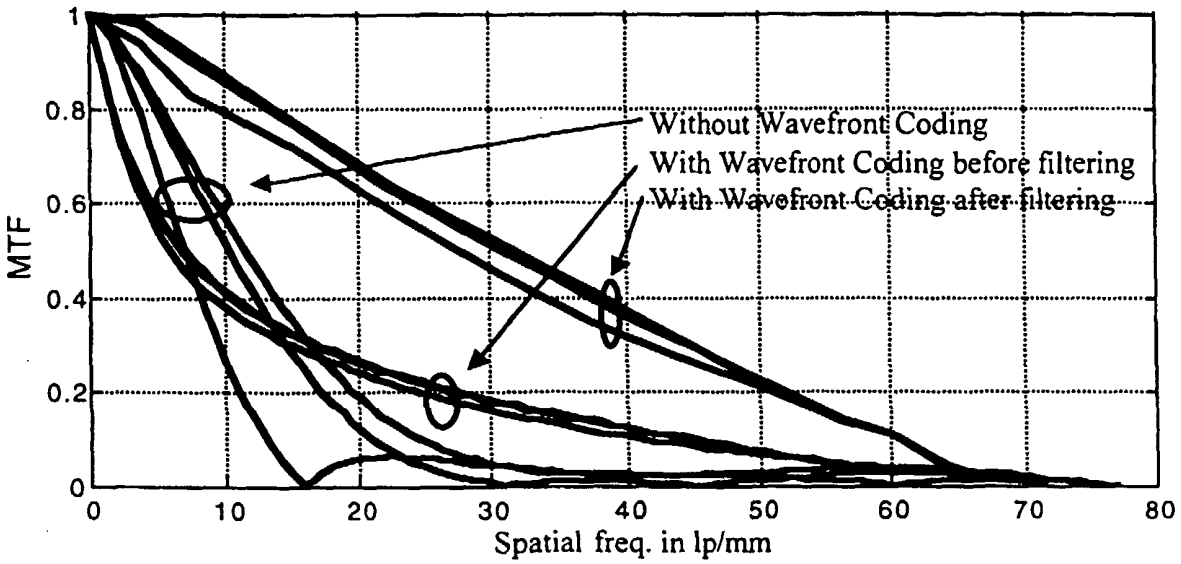
MTF
Spatial freq. in lp/mm
Without Wavefront Coding
With Wavefront Coding before filtering
With Wavefront Coding after filtering
0
0.2
0.4
0.6
0.8
1
0
10
20
30
40
50
60
70
80

Figure 10

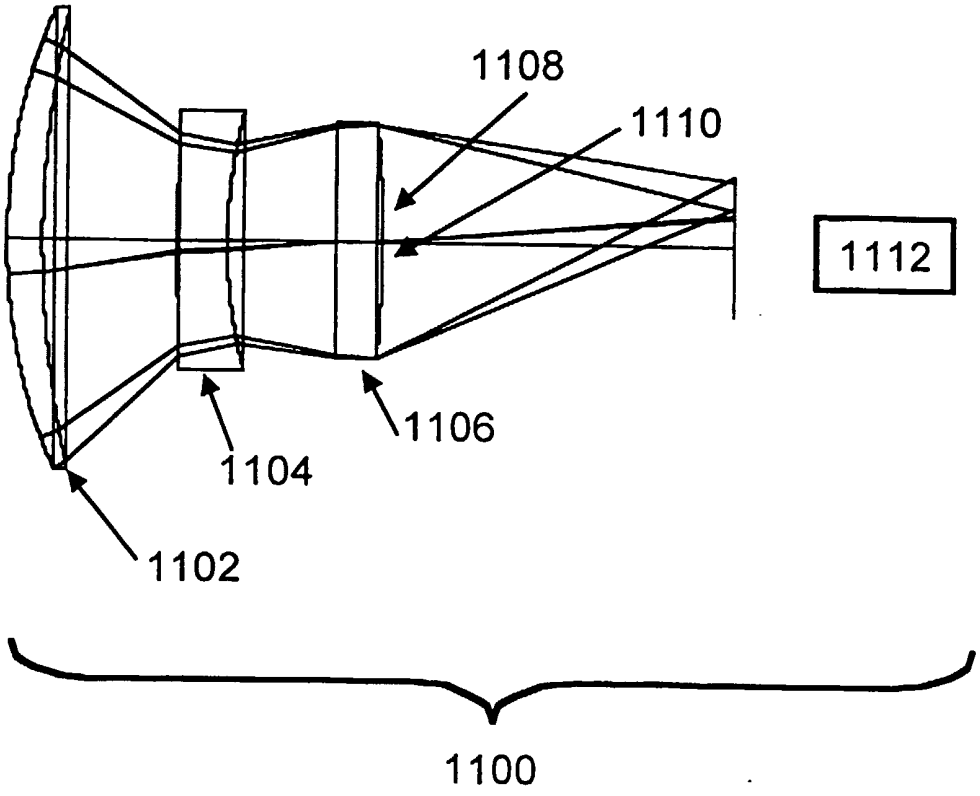

Figure 11

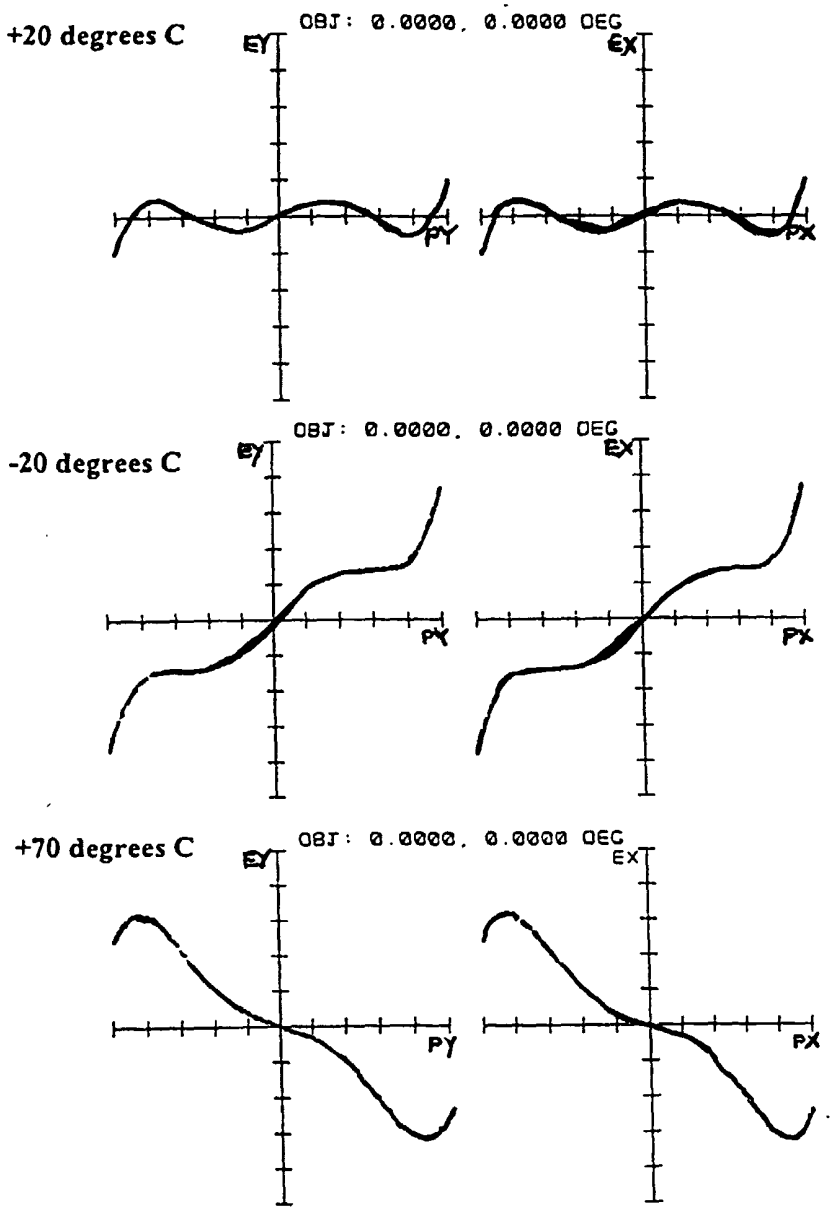
+20 degrees C
OBJ: 0.0000, 0.0000 DEG
EY
EX
PY
PX
-20 degrees C
OBJ: 0.0000, 0.0000 DEG
EY
EX
PY
PX
+70 degrees C
OBJ: 0.0000, 0.0000 DEG
EY
EX
PY
PX

Figure 12

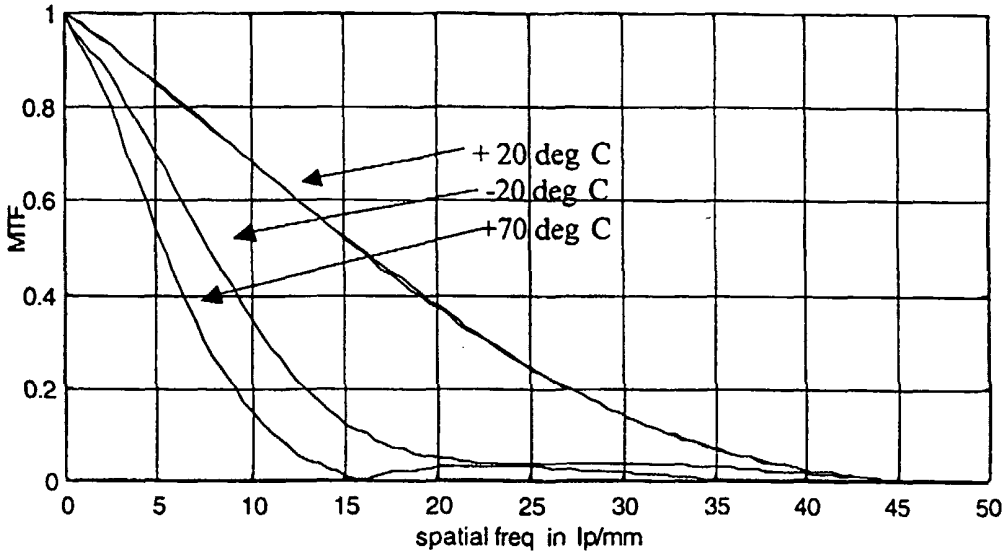
1
0.8
0.6
0.4
0.2
0
MTF
0
5
10
15
20
25
30
35
40
45
50
spatial freq in lp/mm
+ 20 deg C
-20 deg C
+70 deg C

Figure 13

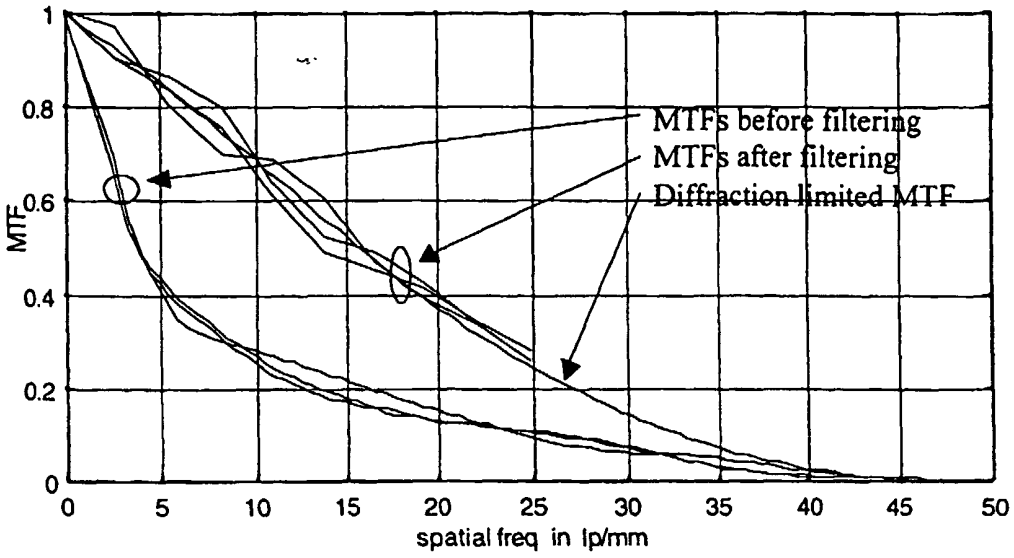
MTFs before filtering
MTFs after filtering
Diffraction limited MTF
MTF
spatial freq in lp/mm
0
0.2
0.4
0.6
0.8
1
0
5
10
15
20
25
30
35
40
45
50

Figure 14

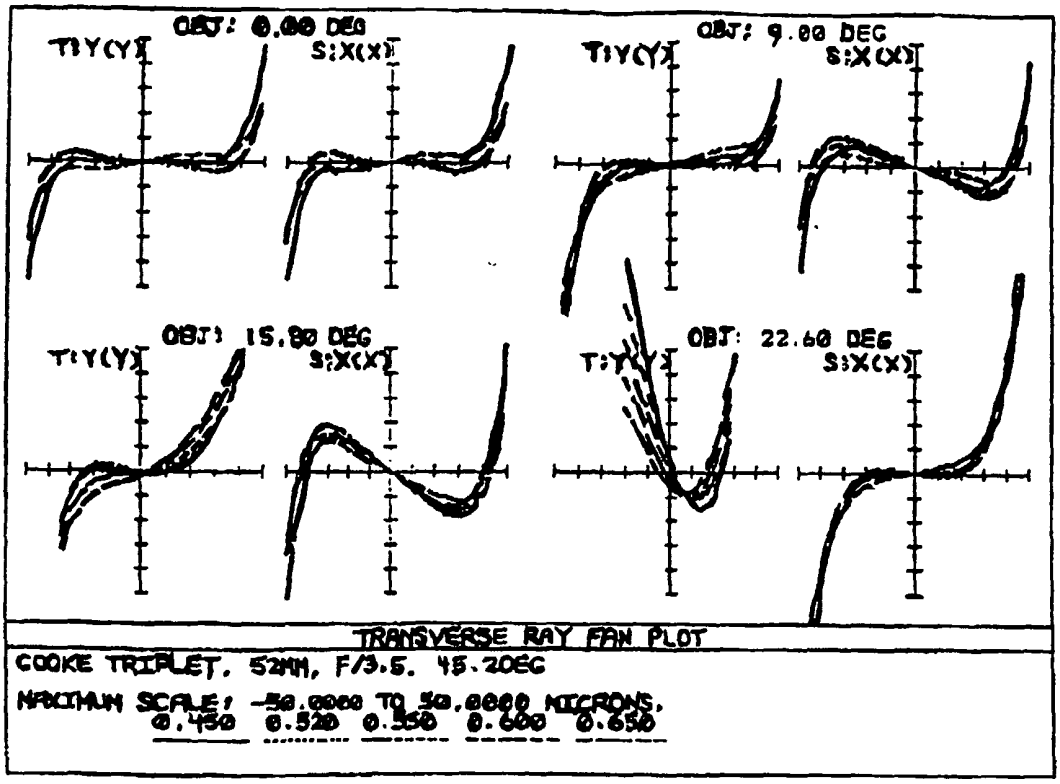
OBJ: 0.00 DEG
T:Y(Y)
S:X(X)
OBJ: 9.00 DEG
T:Y(Y)
S:X(X)
OBJ: 15.80 DEG
T:Y(Y)
S:X(X)
OBJ: 22.60 DEG
T:Y(Y)
S:X(X)
TRANSVERSE RAY FAN PLOT
COOKE TRIPLET, 52MM, F/3.5, 45.20EG
MAXIMUM SCALE: -50.0000 TO 50.0000 MICRONS.
0.450 0.520 0.550 0.600 0.650

Figure 15A

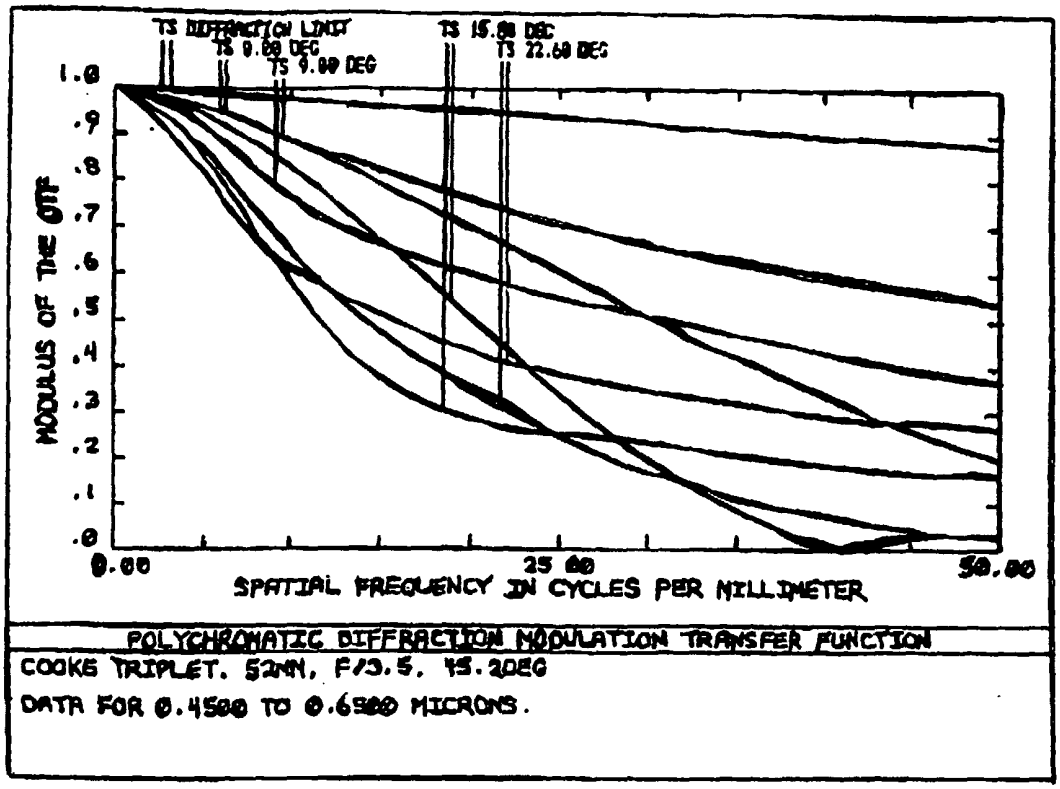
TS DIFFRACTION LIMIT
TS 9.00 DEG
TS 9.00 DEG
TS 15.00 DEG
TS 22.60 DEG
1.0
.9
.8
.7
.6
.5
.4
.3
.2
.1
.0
MODULUS OF THE OTF
0.00
25.00
50.00
SPATIAL FREQUENCY IN CYCLES PER MILLIMETER
POLYCHROMATIC DIFFRACTION MODULATION TRANSFER FUNCTION
COOKE TRIPLET. 52MM, F/3.5. 15.20EG
DATA FOR 0.4500 TO 0.6500 MICRONS.

Figure 15B

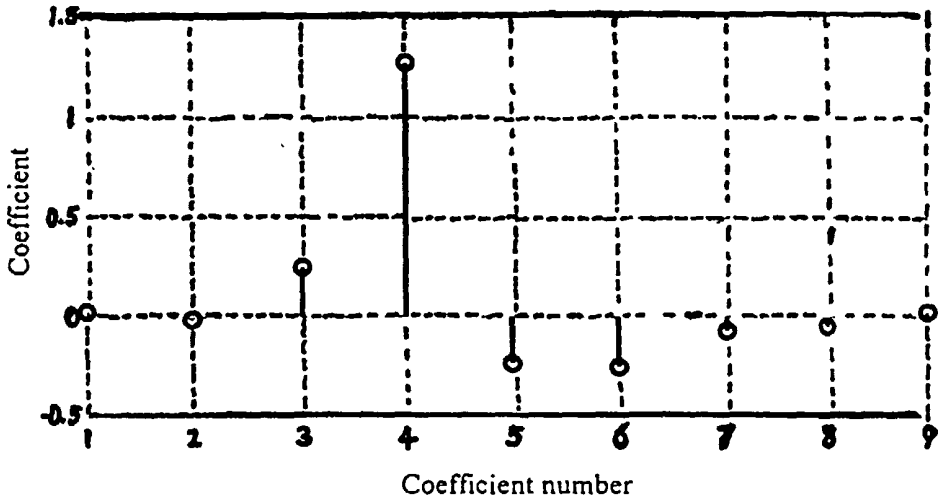

Figure 16

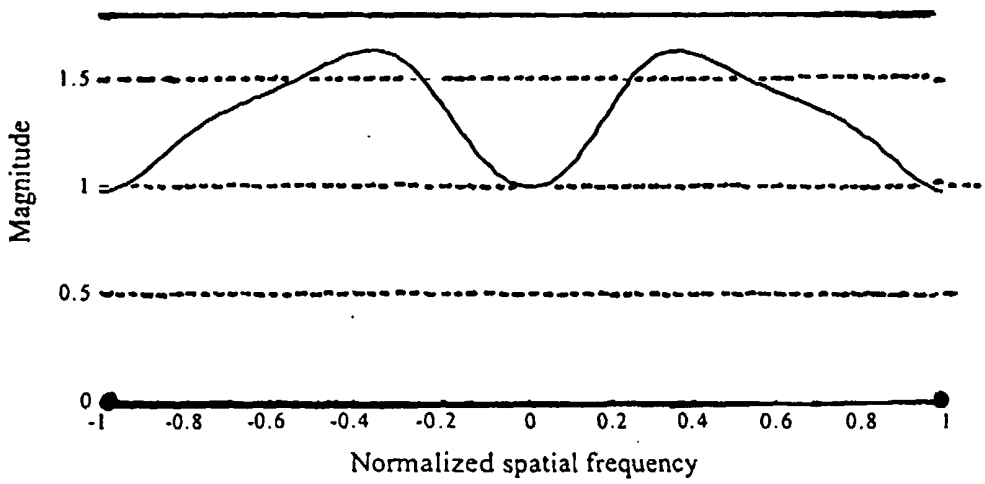
Magnitude
1.5
1
0.5
0
-1
-0.8
-0.6
-0.4
-0.2
0
0.2
0.4
0.6
0.8
1
Normalized spatial frequency

Figure 17